Astron. Astrophys. 282, 304–314 (1994)

ASTRONOMY
AND
ASTROPHYSICS

Multidimensional relativistic hydrodynamics: characteristic fields and modern high-resolution shock-capturing schemes

J.A. Font[1], **J. Mª. Ibáñez**[1], **A. Marquina**[2], **and J. Mª. Martí**[1,3]

[1] Departamento de Física Teórica, Universidad de Valencia, E-46100 Burjassot, Valencia, Spain
[2] Departamento de Matemática Aplicada y Astronomía, Universidad de Valencia, E-46100 Burjassot, Valencia, Spain
[3] Max-Planck-Institut für Astrophysik, Karl-Schwarzschild Str. 1, D-85748 Garching bei München, Germany

Received March 17, accepted June 17, 1993

Abstract. We have derived the spectral decomposition of the Jacobian matrices associated to the fluxes of the three-dimensional special relativistic hydrodynamics system of equations. The interest of this analysis, both from the theoretical and from the numerical point of view, is discussed. We have extended *modern high-resolution shock-capturing methods* to the multidimensional relativistic hydrodynamics as the natural prolongation of our previous work in the one-dimensional case. Two severe tests show the performance of our numerical proposal.

Key words: hydrodynamics – methods: numerical – relativity – shock waves

1. Introduction

Simulations of relativistic flows are currently a topic of increasing interest in several areas of physics such as astrophysics, nuclear physics or plasma physics.

Several astrophysical scenarios involving relativistic flows are, for example, the following: (i) the high-velocity outflows which can be found in galactic jets (Begelman et al. 1984), (ii) the collapse of iron cores of massive stars which activates the Supernovae II explosions and where velocities higher than 0.2 times the speed of light are reached (Brown et al. 1982), or (iii) accretion onto compact objects (Shapiro & Teukolsky 1983). In galactic jets the fluid flow reaches the ultrarelativistic regime (i.e. bulk Lorentz factors greater than 2). The existence of strong gravitational fields in some of the above astrophysical scenarios complicates the problem making a fully general-relativistic description necessary.

A common feature connected with the above astrophysical scenarios is the presence of strong shocks. Relativistic shocks are, from the physical point of view, very important in several problems which also arise in other areas of Physics: (i) Several theories of galaxy formation in Cosmology call for the presence of strong shocks (Miller & Pantano 1989). (ii) Magnetoacoustic shock waves with speeds of up to $4\,10^8$ cm s^{-1} have been achieved in experiments in Plasma Physics (Taussig 1973). (iii) To look for constraints on the nuclear equation of state (EOS) is one of the lines of research followed by experimentalists working with heavy ion reactions. The existence and implications of relativistic shock waves have been considered by theorists in this field of Nuclear Physics (Strottman 1989).

From the numerical point of view the correct modelling of shocks has attracted the attention of many researchers in Astrophysics and in Computational Fluid Dynamics. A numerical scheme in conservation form allows for *shock-capturing*, i.e. it guarantees the correct jump conditions across discontinuities. Traditionally, shock-capturing methods introduced *artificial viscosity* terms in the scheme in order to damp the oscillations and instabilities associated with the numerical computation of discontinuities. Historically, researchers working in relativistic – both special and general – hydrodynamics (see, for example, Nakamura et al. 1980; Piran 1980; Nakamura 1981; Nakamura & Sato 1982; Hawley et al. 1984; Centrella & Wilson 1984; Evans 1986; Stark & Piran 1987), following Wilson's pioneering work (Wilson 1972; Wilson 1979), have used a combination of artificial viscosity and upwind techniques in order to get numerical solutions of the relativistic hydrodynamic equations.

Wilson wrote the system as a set of advection equations. In order to do this, he had to treat terms containing derivatives (in space or time) of the pressure as source terms. This procedure breaks – physically and numerically – an important property of the relativistic hydrodynamics system of equations: its *conservative* character (see below). Wilson's procedure has been extensively applied to the study of many astrophysical scenarios (axisymmetric stellar collapse, numerical cosmology, accretion onto compact objects,...) and proved to be appropriate to describe flows with Lorentz factors up to 2 but, unfortunately, it cannot overcome the ultrarelativistic limit.

Send offprint requests to: J. Mª. Ibáñez

In recent years, the interest in improving the performance reached in relativistic calculations has triggered the development of codes based on other techniques. In this way, Mann (1991) has written a multidimensional general-relativistic hydrodynamical code based on the smooth particle hydrodynamics (SPH) method. However, Mann's results draw us to the conclusion that the SPH method is still far from being able to model ultrarelativistic flows. Analogously, Dubal (1991) has developed a two-dimensional magnetohydrodynamics code using an explicit second-order Lax-Wendroff scheme incorporating a flux-corrected-transport algorithm. When tested against one-dimensional shock tubes the code has shown a performance similar to that of Wilson's code.

On the other hand, during the last decade and after the seminal papers by Godunov (1959) and Van Leer (1979), a number of new shock-capturing finite difference approximations have been constructed and found to be very useful in the numerical simulation of classical (Newtonian) fluid dynamics (see, for example, surveys by Yee 1989 and LeVeque 1991 and references cited therein). In addition to conservation form, these schemes are usually designed to have the following properties: (a) Stable and sharp discrete shock profiles. (b) High accuracy in smooth regions of the flow.

Schemes with these characteristics are usually known as *high-resolution schemes*. They avoid the use of artificial viscosity terms when treating discontinuities and, after extensive experimentation, they appear to be a solid alternative to classical methods with artificial viscosity.

In a previous work, Martí et al. (1991, hereafter MIM) have extended some recent high-resolution shock-capturing (HRSC) methods to solve the relativistic hydrodynamics system of equations in one spatial dimension. Our procedure rested on two main points: (1) To write the equations of relativistic hydrodynamics as a system of *conservation laws* and identify the suitable vector of unknowns. (2) An *approximate Riemann solver* built up from the spectral decomposition of the Jacobian matrix of the system at the boundaries of each numerical cell.

The results obtained in several tests including ultrarelativistic flows and strong shock waves (see MIM and Marquina et al. 1992) have encouraged us to develop a multidimensional version of our previous one-dimensional work. This paper sets out the theoretical and technical ingredients which are necessary for a proper extension of HRSC methods to multidimensional relativistic hydrodynamics. In order to check our hydro-code we have chosen two severe tests. For one of them, *the steady relativistic oblique shock*, exact analytical solution exists (Königl 1980). Preliminary results on these tests can also be found in Ibáñez (1993).

Our analysis has been performed in Minkowski spacetime and using Cartesian coordinates, although it can be easily generalized to other coordinates (in Minkowski space-time) and general space-times described by a diagonal metric tensor. In these cases the spectral decomposition of the Jacobian matrices can be trivially extended as we have shown in the one-dimensional case (see MIM).

Finally, when this work was written, we have been aware of the work of Eulderink & Mellema (1993) in which similar techniques have been applied to the study of the confinement of astrophysical jets.

Present paper is organized as follows. Section 2 is devoted to the analysis of the relativistic hydrodynamics system of equations as a system of conservation laws. In this section, we write the multidimensional equations of relativistic hydrodynamics in conservation form and define the appropriate set of unknowns. In Sect. 3 we derive the spectral decomposition of the Jacobian matrices associated to the fluxes in each spatial direction. Two severe tests of our multidimensional code are displayed in Sect. 4. This section also contains other comments related with our numerical code. Finally, main conclusions are presented in Sect. 5.

2. Relativistic hydrodynamics as a system of conservation laws

A one-dimensional *hyperbolic system of conservation laws* is

$$\frac{\partial \boldsymbol{u}}{\partial t} + \frac{\partial \boldsymbol{f}(\boldsymbol{u})}{\partial x} = 0 \,, \tag{1}$$

where $\boldsymbol{u}$ is the N-dimensional vector of unknowns and $\boldsymbol{f}(\boldsymbol{u})$ are N vector-valued functions called *fluxes*. The above system (1) is hyperbolic if the Jacobian matrix

$$\boldsymbol{A} = \frac{\partial \boldsymbol{f}(\boldsymbol{u})}{\partial \boldsymbol{u}} \tag{2}$$

has real and distinct eigenvalues $\{\lambda_n(\boldsymbol{u})\}_{n=1,\ldots N}$ and the set of eigenvectors is complete in $\mathcal{R}^N$. If some of the eigenvalues are equal the system is said to be non-strictly hyperbolic. The equation

$$\mathrm{d}x/\mathrm{d}t = \lambda_n(\boldsymbol{u}) \tag{3}$$

defines the nth *characteristic field*.

The equations describing the evolution of a relativistic fluid are *local conservation laws*: the local conservation of baryon number density

$$\nabla_\mu J^\mu = 0 \tag{4}$$

and the local conservation of energy-momentum

$$\nabla_\mu T^{\mu\nu} = 0 \tag{5}$$

(throughout this paper, Greek indices run from 0 to 3 and the Einstein summation convention is used), the current J^μ and the energy-momentum tensor $T^{\mu\nu}$ being

$$J^\mu = \rho u^\mu \,, \tag{6}$$

$$T_{\mu\nu} = \rho h u_\mu u_\nu + p g_{\mu\nu} \,. \tag{7}$$

In the above equations ρ is the rest-mass density, p is the pressure and h is the specific enthalpy, defined by $h = 1 +$

$\varepsilon + p/\rho$, where ε is the specific internal energy. u^μ is the four-velocity of the fluid and $g_{\mu\nu}$ defines the metric of the space-time $\mathcal{M}$ where the fluid evolves. ∇_μ stands for the covariant derivative.

The expression chosen for the energy-momentum tensor restricts it to a perfect fluid and, therefore, we do not take heat conduction, viscous interactions or magnetic fields into account.

In Minkowski space-time and using Cartesian coordinates ($x^\mu = \{t, x, y, z\}$), the above system of Eqs. (4) and (5), can be written in a more compact way as:

$$\frac{\partial \boldsymbol{F}^\mu(\boldsymbol{w})}{\partial x^\mu} = 0, \tag{8}$$

where the five-vector of unknowns is

$$\boldsymbol{w} = (\rho, v^x, v^y, v^z, \varepsilon) \tag{9}$$

and the quantities $\boldsymbol{F}^\alpha$ are

$$\boldsymbol{F}^0(\boldsymbol{w}) = (\rho W, \rho h W^2 v^x, \rho h W^2 v^y, \rho h W^2 v^z, \rho h W^2 - p - \rho W), \tag{10}$$

$$\boldsymbol{F}^i(\boldsymbol{w}) = (\rho W v^i, \rho h W^2 v^i v^x + p\delta^{ix}, \rho h W^2 v^i v^y + p\delta^{iy}, \rho h W^2 v^i v^z + p\delta^{iz}, \rho h W^2 v^i - \rho W v^i) \tag{11}$$

($i = x, y, z$).

In the above expressions, the components of the three-velocity, v^i, are defined according to $v^i \equiv u^i/u^0$ and the Lorentz factor, defined by $W \equiv u^0$, satisfies the familiar relation $W = (1 - \boldsymbol{v}^2)^{-1/2}(\boldsymbol{v}^2 = (v^x)^2 + (v^y)^2 + (v^z)^2)$. The components of $\boldsymbol{F}^0(\boldsymbol{w})$ are, respectively, the relativistic rest-mass density, the three components of the relativistic momentum density and the total energy density.

An equation of state $p = p(\rho, \varepsilon)$ closes, as usual, the system. A very important quantity derived from the equation of state is the local sound velocity c_s:

$$hc_s^2 = \chi + (p/\rho^2)\kappa, \tag{12}$$

with $\chi = \partial p/\partial \rho$ and $\kappa = \partial p/\partial \epsilon$.

Introducing the Jacobian matrices $\mathcal{A}^\alpha(\boldsymbol{w})$ associated to the five-vectors $\boldsymbol{F}^\alpha(\boldsymbol{w})$

$$\mathcal{A}^\alpha = \frac{\partial \boldsymbol{F}^\alpha(\boldsymbol{w})}{\partial \boldsymbol{w}}, \tag{13}$$

system (8) can be written as a quasi-linear system of first order partial differential equations for the unknown field $\boldsymbol{w}$

$$\mathcal{A}^\mu(\boldsymbol{w})\frac{\partial \boldsymbol{w}}{\partial x^\mu} = 0. \tag{14}$$

The explicit expressions of matrices $\mathcal{A}^\alpha$ have been displayed in Appendix A. Finally, we introduce the vectors

$$\boldsymbol{u} = \boldsymbol{F}^0(\boldsymbol{w}) \tag{15}$$

(the three-dimensional counterpart of the unknown field vector in MIM; see expression (12) of that paper) and

$$\boldsymbol{f}^i = \boldsymbol{F}^i \circ (\boldsymbol{F}^0)^{-1} \tag{16}$$

($i = 1, 2, 3$) where $\circ$ means composition of functions and $(\cdot)^{-1}$ stands for the inverse function.

With the above definitions, system (8) reads as a system of conservation laws, in the sense of Lax (1973), for the new vector of unknowns $\boldsymbol{u}$

$$\frac{\partial \boldsymbol{u}}{\partial x^0} + \frac{\partial \boldsymbol{f}^i(\boldsymbol{u})}{\partial x^i} = 0. \tag{17}$$

In the above system (17) we can define three 5×5-Jacobian matrices $\mathcal{B}^i(\boldsymbol{u})$, the Jacobian matrices associated to the vector $\boldsymbol{f}^i(\boldsymbol{u})$, the *flux* in the i-direction of the system (17) as:

$$\mathcal{B}^i = \frac{\partial \boldsymbol{f}^i(\boldsymbol{u})}{\partial \boldsymbol{u}}. \tag{18}$$

A routine calculation shows that

$$\mathcal{B}^i = \mathcal{A}^i(\mathcal{A}^0)^{-1}. \tag{19}$$

In order to apply HRSC methods to solve the equations of relativistic hydrodynamics as written in (17), the knowledge of the spectral decomposition of the Jacobian matrices $\mathcal{B}^i$ is crucial. The next section is devoted to this purpose.

3. Characteristic fields

The hyperbolic character of relativistic hydrodynamics has been exhaustively studied by Anile and collaborators (see Anile 1989, and references cited therein) by applying the Friedrichs' definition of hyperbolicity (Friedrichs 1974) to the system of equations in the form of a quasi-linear system [expression (14)]. According to this definition, system (14) will be hyperbolic in the time-direction defined by the vector field ξ with $\xi_\alpha \xi^\alpha = -1$, if the following two conditions hold:

(i) det $(\mathcal{A}^\alpha \xi_\alpha) \neq 0$,

(ii) for any ζ such that $\zeta_\alpha \xi^\alpha = 0$, $\zeta_\alpha \zeta^\alpha = 1$, the eigenvalue problem

$$\mathcal{A}^\alpha(\zeta_\alpha - \lambda \xi_\alpha)\boldsymbol{r} = 0 \tag{20}$$

has only real eigenvalues $\{\lambda_n\}_{n=1,\dots 5}$ and a complete set of eigenvectors $\{\boldsymbol{r}_n\}_{n=1,\dots 5}$.

Besides verifying the hyperbolic character of the relativistic hydrodynamics, Anile and collaborators have obtained the explicit expressions for the eigenvalues and eigenvectors of problem (20) in the *local rest frame*, characterized by

$$u^\mu = \delta^\mu_0. \tag{21}$$

We have redone the calculations in an arbitrary reference frame in which the motion of the fluid is described by the four-velocity

$$u^\mu = W(1, v^i). \tag{22}$$

Let us focus on one spatial direction $x^1 = x$ and make the following choice for the vectors $\xi^\alpha = (1, 0, 0, 0)$ and

$\zeta^\alpha = (0, 1, 0, 0)$ (the analysis in the other two spatial directions can be performed in the same way). Now, the above condition (ii) becomes

$$(\mathcal{A}^1 - \lambda\mathcal{A}^0)\boldsymbol{r} = 0 \tag{23}$$

and leads, after straightforward computations, to the following eigenvalues associated with the so-called *acoustic waves*

$$\lambda_\pm = \frac{1}{1-\boldsymbol{v}^2 c_s^2}\Big\{v^x(1-c_s^2) \pm c_s\sqrt{(1-\boldsymbol{v}^2)[1-(v^x)^2-((v^y)^2+(v^z)^2)c_s^2]}\Big\} \tag{24}$$

and

$$\lambda_0 = v^x \text{(triple)}, \tag{25}$$

for the *material waves*.

A complete set of right-eigenvectors of the problem (23) is

$$\boldsymbol{r}_0 = \left\{\begin{array}{l}(-\kappa,0,0,0,\chi)\\(-\kappa,0,1,0,\chi)\\(-\kappa,0,0,1,\chi)\end{array}\right\}, \tag{26}$$

$$\boldsymbol{r}_\pm = \begin{bmatrix}1\\(v^x-\lambda_\pm)(1-\lambda_\pm v^x)/\rho\Delta_\pm\\-\lambda_\pm v^y(v^x-\lambda_\pm)/\rho\Delta_\pm\\-\lambda_\pm v^z(v^x-\lambda_\pm)/\rho\Delta_\pm\\-\chi/\kappa-h(v^x-\lambda_\pm)^2W^2/\kappa\Delta_\pm\end{bmatrix} \tag{27}$$

with

$$\Delta_\pm = -\boldsymbol{v}^2W^2\lambda_\pm^2 + 2v^xW^2\lambda_\pm - [1+(v^x)^2W^2], \tag{28}$$

which is always different from zero for real values of $\lambda_\pm$.

Several comments should be made:

(i) In the case ($v^x = v$, $v^y = v^z = 0$), expression (24) gives the corresponding one-dimensional eigenvalues (see MIM):

$$\lambda_\pm = \frac{v \pm c_s}{1 \pm vc_s}. \tag{29}$$

(ii) In the limit $|v^x| \longrightarrow 1$, the *genuinely nonlinear* characteristic fields $\lambda_\pm$ become *linearly degenerate*.

The previous analysis is interesting for our purpose of obtaining the spectral decomposition of matrices $\mathcal{B}^i$ bearing in mind that, if $\{\lambda_n, \boldsymbol{r}_n\}_{n=1,\dots5}$ are, respectively, the eigenvalues and eigenvectors of problem (23), then the corresponding eigenvalues and eigenvectors of $\mathcal{B}^i$, $\{\lambda_n^*, \boldsymbol{r}_n^*\}_{n=1,\dots5}$, are:

$$\{\lambda_n^*, \boldsymbol{r}_n^*\}_{n=1,\dots5} = \{\lambda_n, \mathcal{A}^0\boldsymbol{r}_n\}_{n=1,\dots5}. \tag{30}$$

The proof of this statement is shown in Appendix B.

4. Multidimensional relativistic tests

In this section we present numerical results obtained in two severe tests which are standard in multidimensional Newtonian fluid dynamics: (1) the relativistic *oblique shock*, and (2) the relativistic *Emery's step*.

Our code is based on a finite discretization of the equations of relativistic hydrodynamics in conservation form (17). Using a *method of lines*, this discretization reads:

$$\frac{\mathrm{d}\boldsymbol{u}_{i,j,k}(t)}{\mathrm{d}t} = -\frac{\hat{\boldsymbol{f}}_{i+\frac12,j,k}-\hat{\boldsymbol{f}}_{i-\frac12,j,k}}{\Delta x} - \frac{\hat{\boldsymbol{g}}_{i,j+\frac12,k}-\hat{\boldsymbol{g}}_{i,j-\frac12,k}}{\Delta y} - \frac{\hat{\boldsymbol{h}}_{i,j,k+\frac12}-\hat{\boldsymbol{h}}_{i,j,k-\frac12}}{\Delta z}, \tag{31}$$

where subscripts i, j, k are related, respectively, with x, y and z-discretizations, and refer to cell-centered quantities. Δx, Δy and Δz represent the cell width in the three coordinate directions.

Quantities $\hat{\boldsymbol{f}}_{i+\frac12,j,k}$, $\hat{\boldsymbol{g}}_{i,j+\frac12,k}$ and $\hat{\boldsymbol{h}}_{i,j,k+\frac12}$ are the *numerical fluxes* at the cell interfaces, calculated with an approximate Riemann solver based on the spectral decomposition of the corresponding Jacobian matrix. For the numerical fluxes in the x-direction we have:

$$\hat{\boldsymbol{f}}_{i+\frac12,j,k} = \frac12\Big(\boldsymbol{f}(\boldsymbol{u}^{\mathrm{L}}_{i,j,k}) + \boldsymbol{f}(\boldsymbol{u}^{\mathrm{R}}_{i+1,j,k}) - \sum_{n=1}^{5} |\tilde{\lambda}_n| \Delta\tilde{\omega}_n \tilde{\boldsymbol{r}}^*_n\Big), \tag{32}$$

where $\boldsymbol{u}^{\mathrm{L}}_{i,j,k}$ and $\boldsymbol{u}^{\mathrm{R}}_{i+1,j,k}$ stand for the left and right states of the interface $i+\frac12$ and have been obtained by using a *monotonic linear reconstruction* of the cell-centered values (Van Leer, 1979) in order to achieve second-order spatial accuracy. $\{\tilde{\lambda}_n, \tilde{\boldsymbol{r}}^*_n\}_{n=1,\dots5}$ are, respectively, the eigenvalues and eigenvectors of the Jacobian matrix $\mathcal{B}^1$ calculated at the interface $i+\frac12$ through some average of $\boldsymbol{u}^{\mathrm{L}}_{i,j,k}$ and $\boldsymbol{u}^{\mathrm{R}}_{i+1,j,k}$. Finally, the quantities $\{\Delta\tilde{\omega}_n\}_{n=1,\dots5}$, the jumps of the local characteristic variables across each characteristic field, are obtained from:

$$\boldsymbol{u}^{\mathrm{R}}_{i+1,j,k} - \boldsymbol{u}^{\mathrm{L}}_{i,j,k} = \sum_{n=1}^{5} \Delta\tilde{\omega}_n \boldsymbol{r}^*_n. \tag{33}$$

The advance in time has been performed by means of a third-order Runge-Kutta method that preserves the conservation form of the scheme and does not increase the total variation of the solution at each time substep (Shu & Osher 1989). Note that we do not perform any spatial splitting. At each time step, an implicit equation for pressure must be solved in order to get the new value of $\boldsymbol{w}$.

The time step is constrained by the CFL (Courant–Friedrichs–Lewy) condition. The CFL condition, necessary for stability, states that the numerical signal speed must be at least as fast as the maximum signal speed (see, for example, Sod 1987). A 2D formulation of this condition is

$$\Delta t = \mathrm{CFL} \times \min\left(\frac{\Delta x}{\frac12(|\lambda^{(1)}_{+i-1/2,j}| - |\lambda^{(1)}_{-i+1/2,j}|)}, \frac{\Delta y}{\frac12(|\lambda^{(2)}_{+i,j-1/2}| - |\lambda^{(2)}_{-i,j+1/2}|)}\right), \tag{34}$$

where $\mathrm{CFL} \leq 1/\sqrt{2}$ (we have taken CFL = 0.5) and $\lambda_{\pm}^{(1)}$ and $\lambda_{\pm}^{(2)}$ are the corresponding eigenvalues associated to the matrices $\mathcal{B}^1$ and $\mathcal{B}^2$, respectively. The above relation (34) expresses the dependence of the time step – and, a fortiori, the CPU time – on the size of the grid. In the numerical experiments shown in present work the computing time is 411μs per grid point and per time step on a IBM 30-9021 VF (only 30% vectorisation). Currently, we are working in a new version of the code which must reduce this computing time in a factor greater than ten.

Finally, given its interest in astrophysical applications, let us make some comments concerning the numerical viscosity of these high-resolution shock-capturing methods. The last term in the numerical flux (32) gives information about the numerical viscosity of the scheme. In the one-dimensional scalar case – and a uniform grid – a general 3-point finite-difference scheme in conservation form has a numerical flux of the form

$$\hat{\boldsymbol{f}}_{i+\frac{1}{2}} = \tfrac{1}{2}[f(u_i) + f(u_{i+1}) - (1/\mu)Q(\xi_{i+\frac{1}{2}})(u_{i+1} - u_i)], \quad (35)$$

where $\mu = \Delta t/\Delta x$, $\xi = \mu a$, $a = \partial f/\partial u$ (except in discontinuities) and $Q(\xi_{i+\frac{1}{2}})$ can be viewed as the viscosity of the scheme (Harten 1983; Osher 1985). Some estimations about the amount of numerical viscosity can be given following the work by Harten (1983). Harten (1983) has studied the influence of numerical viscosity in high-resolution second order accurate TVNI (total variation nonincreasing) schemes (see in this reference for definition and properties of TVNI schemes) and established the following relations:

$$|\,\xi\,| \leq Q(\xi) \leq 1 \quad \text{for} \quad |\,\xi\,| \leq \mathrm{CFL} \leq 1\,. \quad (36)$$

The natural way of extending to systems the above definition of numerical viscosity for scalar equations is by using a local characteristic approach in order to decouple the original system into a set of scalar equations in each characteristic field (Harten 1983). Work in this direction is in progress.

4.1. Relativistic oblique shock

The basic algebraic relations which connect the two states at each side of a steady relativistic oblique shock have been derived by Königl (1980), for ideal gases with a constant adiabatic index Γ, in the local rest-frame of the shock front. A fundamental difference between the Newtonian and relativistic descriptions is the fact that, in the relativistic case, the jump in density, which increases with the upstream velocity, tends to infinity in the extreme-relativistic regime. Königl derives an algebraic equation which defines implicitly the jump in the normal components of velocity $\chi \equiv v_2^{\perp}/v_1^{\perp}$ in terms of the known upstream state (the upstream and downstream regions of the front are denoted by 1 and 2, respectively). Once the quantity χ is calculated the remaining unknowns are easily obtained (see Königl 1980).

We have generated a steady oblique shock throwing an ideal gas with $\Gamma = 7/5$ through a corner (an oblique plane) with a wedge angle of $\tan^{-1}(1/2)$. In the case of an infinite oblique plane, this shock front is also infinite. Moreover, since it makes the same angle with the incoming flow everywhere, its strength is constant and hence the state immediately behind the shock is also constant, allowing us to compare the jumps in the hydrodynamical quantities at both sides of the shock front with the analytical expressions derived by Königl.

The initial density, in our experiments, is 1.4 and the pressure the one resulting for a Mach 3 flow (Newtonian definition). The initial velocity (in units of the speed of light) runs from 0.01 ($W = 1.00$) to 0.95 ($W = 3.21$). A rectangular grid of 120×40 has been used.

The solution looks like the Newtonian one. This can be explained if we take into account that, as several authors (see, for example, Königl 1980; Wilson 1987) have emphasized, the equations of steady special-relativistic gas dynamics and steady non-relativistic gas dynamics have a similar mathematical form, when expressed in suitable variables. This property has been used in order to find numerical solutions for relativistic steady flows.

Figure 1 shows the shock front formed in the case $v_1 = 0.95$. We have plotted nine isodensity curves at regular intervals of width 0.005. In this way we get a resolution fine enough to solve the shock in the range $\rho_2 \in (10.957, 10.912)$. Figure 2 shows the profile of the proper speed of the fluid $u = Wv$ as a function of the x-coordinate parametrized for different values of the y-coordinate. The corner of the wedge is placed at $x = 2$ and the inflexion points of these curves indicate asymptotically the jump in proper speed which would correspond to an infinite obstacle.

In Table 1 we compare our numerical results with the exact solution of Königl. For each value of the initial inflow velocity we have displayed two values of ρ_2, associated to the numerical incertitude pointed above, and their corresponding jumps $\Delta\rho = \rho_2/\rho_1$. The jump in the proper speed $\Delta u = u_2/u_1$ and the numerical values of the angle β between the shock front and the direction of the inflow velocity have been obtained from the analysis of the corresponding figures such as Fig. 2 and Fig. 1, respectively (we have included dispersion bar errors). In order to facilitate the comparison, Table 1 includes two sets of theoretical values spanning the dispersion bar of β. As we can see from this table the values of all variables involved in the problem agree satisfactory with the analytical ones.

4.2. Relativistic Emery's step

A severe test for two-dimensional flows in presence of shocks is the flat-faced step originally introduced by Emery (1968) to compare several difference schemes in classical fluid dynamics: a Mach 3 flow (Newtonian definition) is injected into a tunnel containing a step. The tunnel is 3 units long and 1 unit wide. The step is 0.2 units high and is located 0.6 units from the left-hand end of the tunnel. Slab symmetry is assumed.

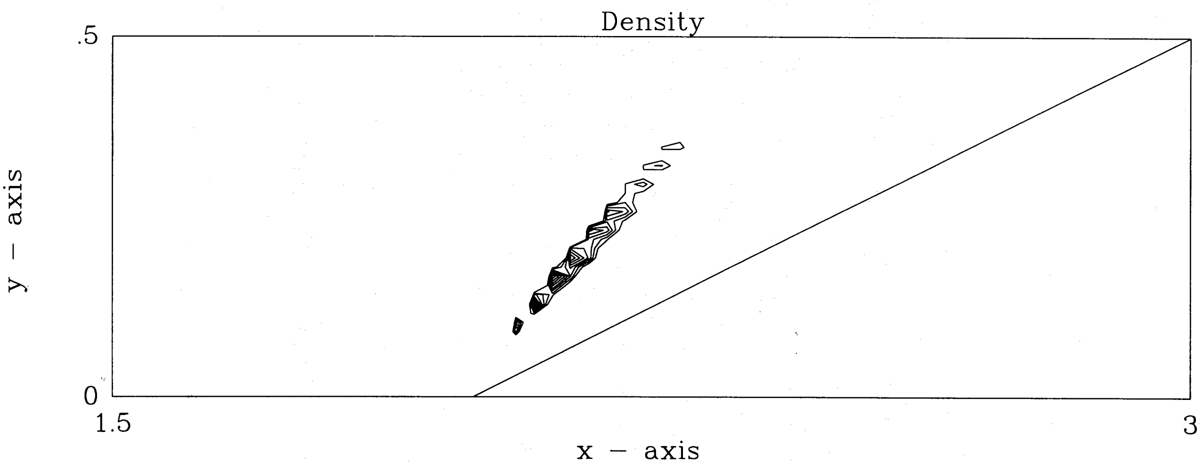

Fig. 1. Steady relativistic oblique shock. Initial inflow velocity 0.95 (in units of the speed of light). Nine isodensity curves have been plotted spanning, regularly, the interval between 10.957 and 10.912

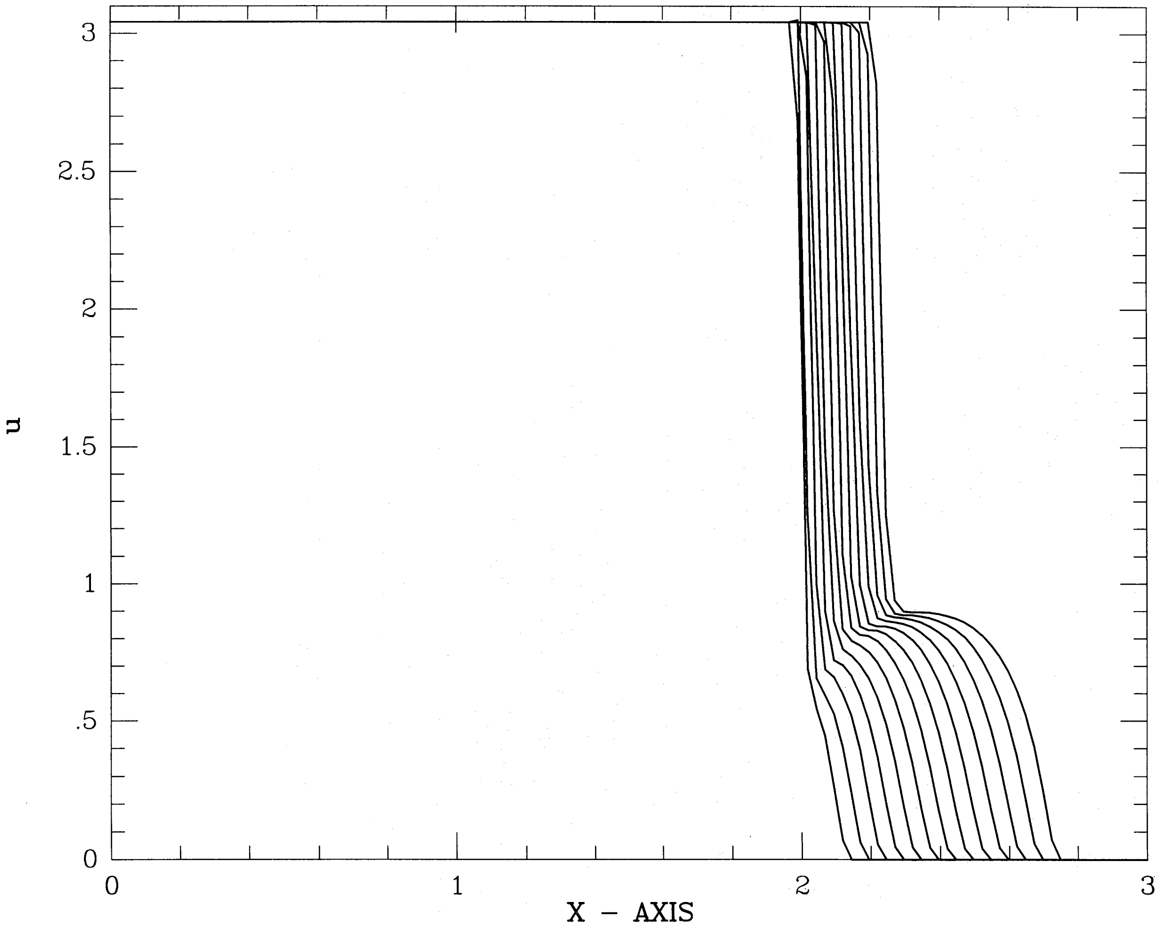

Fig. 2. Flow velocity in the steady relativistic oblique shock problem. Initial inflow velocity 0.95 (in units of the speed of light). The sample of curves is parametrized by the y-coordinate, being the corner placed at $x = 2$.

The boundary conditions are: (1) Reflecting boundary conditions along the walls of the tunnel and at the left face and the top of the step. No additional boundary condition near the corner of the step has been introduced. (2) On the right and the left sides of the tunnel, respectively, outflow and inflow boundary conditions are applied.

The initial conditions for the gas in the tunnel are: $\rho(x, y, 0) = \rho_0 = 1.4$, $v^x(x, y, 0) = v_0^x$ and $v^y(x, y, 0) = v_0^y =$

Table 1. Steady relativistic oblique shock. See text for details about entries

v_1	Numerical results				Analytical relations			
	β	ρ_2	$\Delta\rho$	Δu	β	χ	$\Delta\rho$	Δu
0.01	49.5 ± 0.5	4.319	3.086	0.69 ± 0.01	49	0.3292	3.038	0.702
		4.309	3.078		50	0.3244	3.082	0.689
0.9	45.5 ± 0.5	8.209	5.863	0.423 ± 0.007	45	0.2945	5.829	0.429
		8.184	5.848		46	0.2942	5.902	0.418
0.95	47.5 ± 0.5	10.957	7.826	0.301 ± 0.005	47	0.3034	7.726	0.306
		10.912	7.794		48	0.3038	7.817	0.297

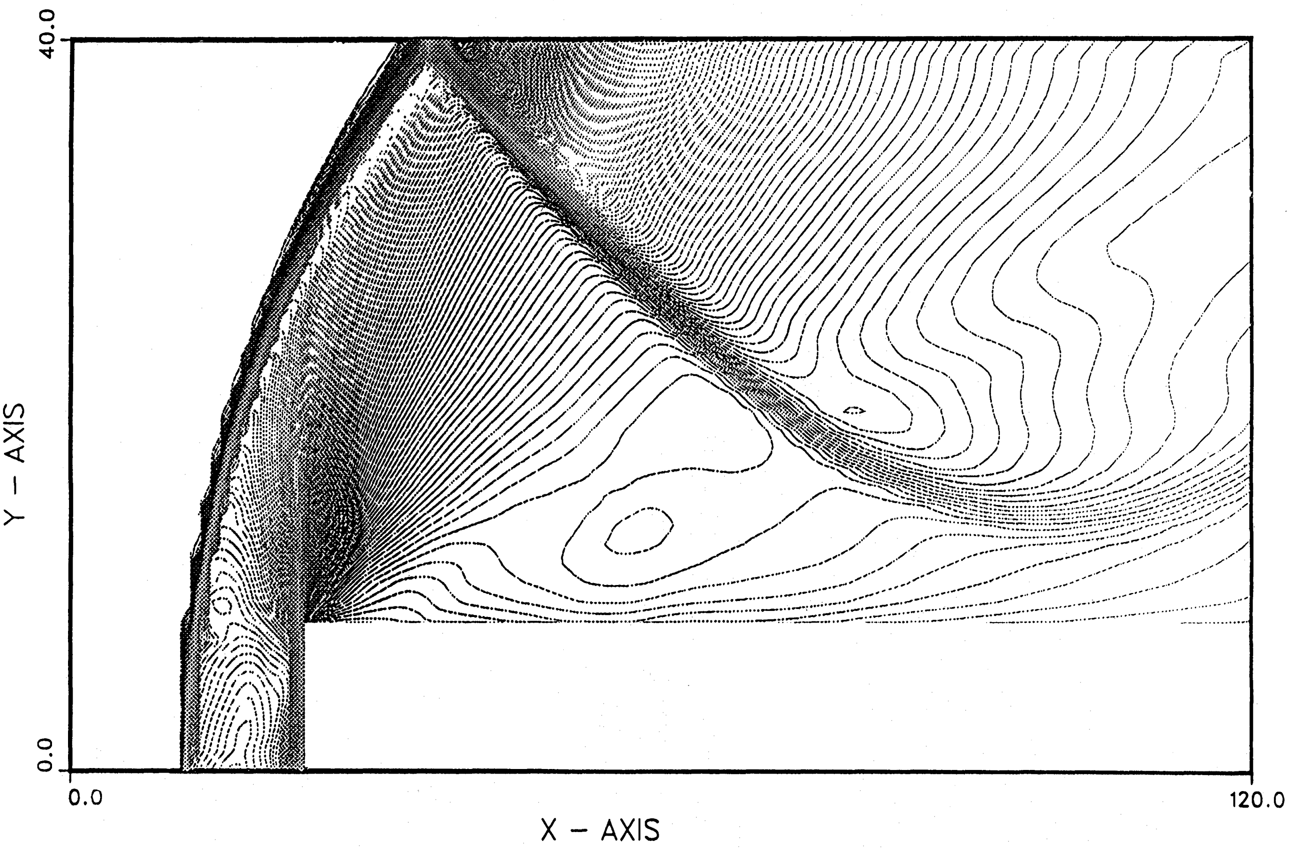

Fig. 3. Relativistic Emery's step. Isodensity curves at $t = 4$, in units of the Courant time

0, for all x, y. The value of the initial pressure is derived from the other variables. The initial value of the x-component of the three-velocity v_0^x has been used as a free parameter for different runs.

The EOS considered is the one of an ideal gas with $\Gamma = 7/5$. Gas is continually fed in at the left-hand boundary with the flow variables given by their initial values. A rectangular grid of 120×40 has been used.

At the transonic rarefactions, where solutions violating entropy may develop (and, in fact, it does), an entropy viscosity term according to the prescription of Harten & Hyman (1983) was incorporated.

Figures 3–5 show the isodensity curves of the system (inflow velocity $v_0^x = 0.9$; $W = 2.29$) at three points in its evolution ($t = 4$–6, in units of the Courant time) before the steady solution has been reached and when the flow ex-

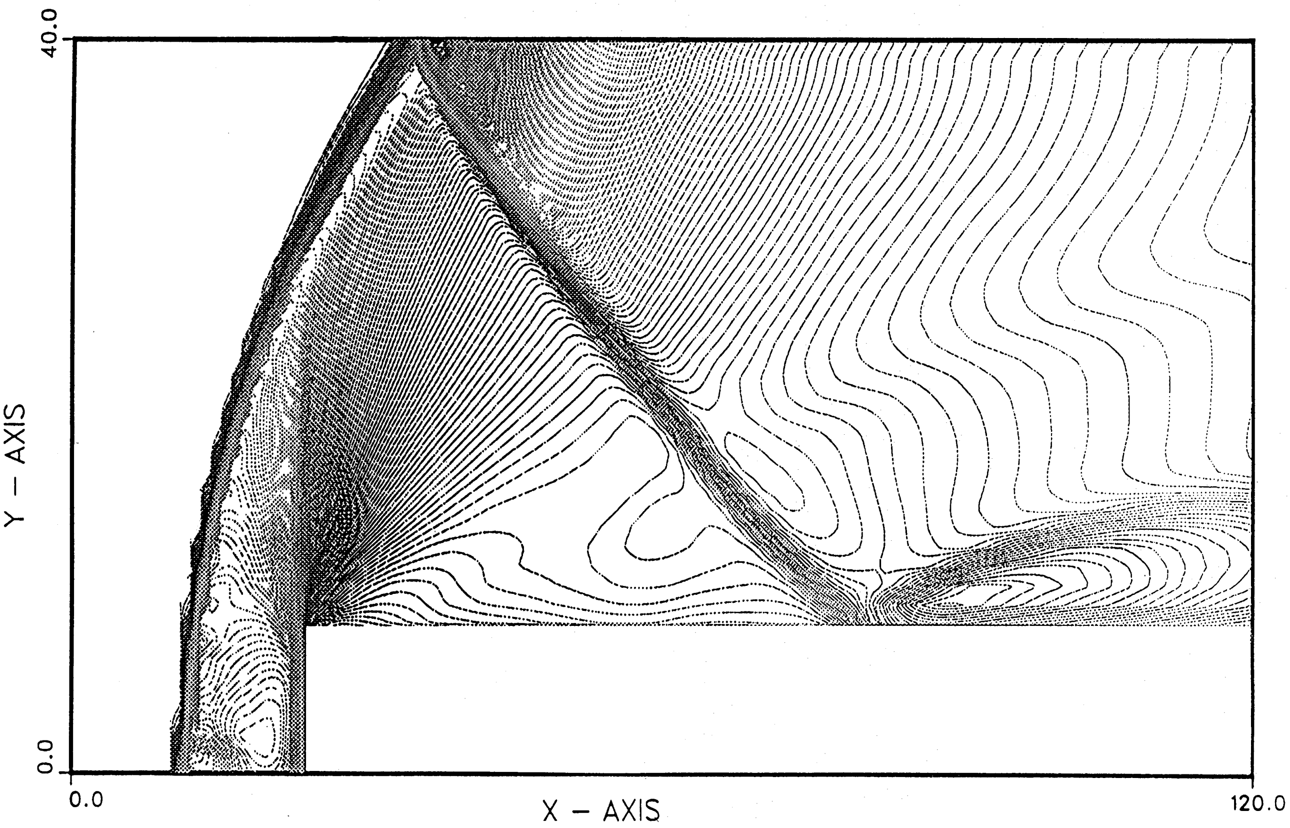

Fig. 4. Relativistic Emery's step. Isodensity curves at $t = 5$, in units of the Courant time

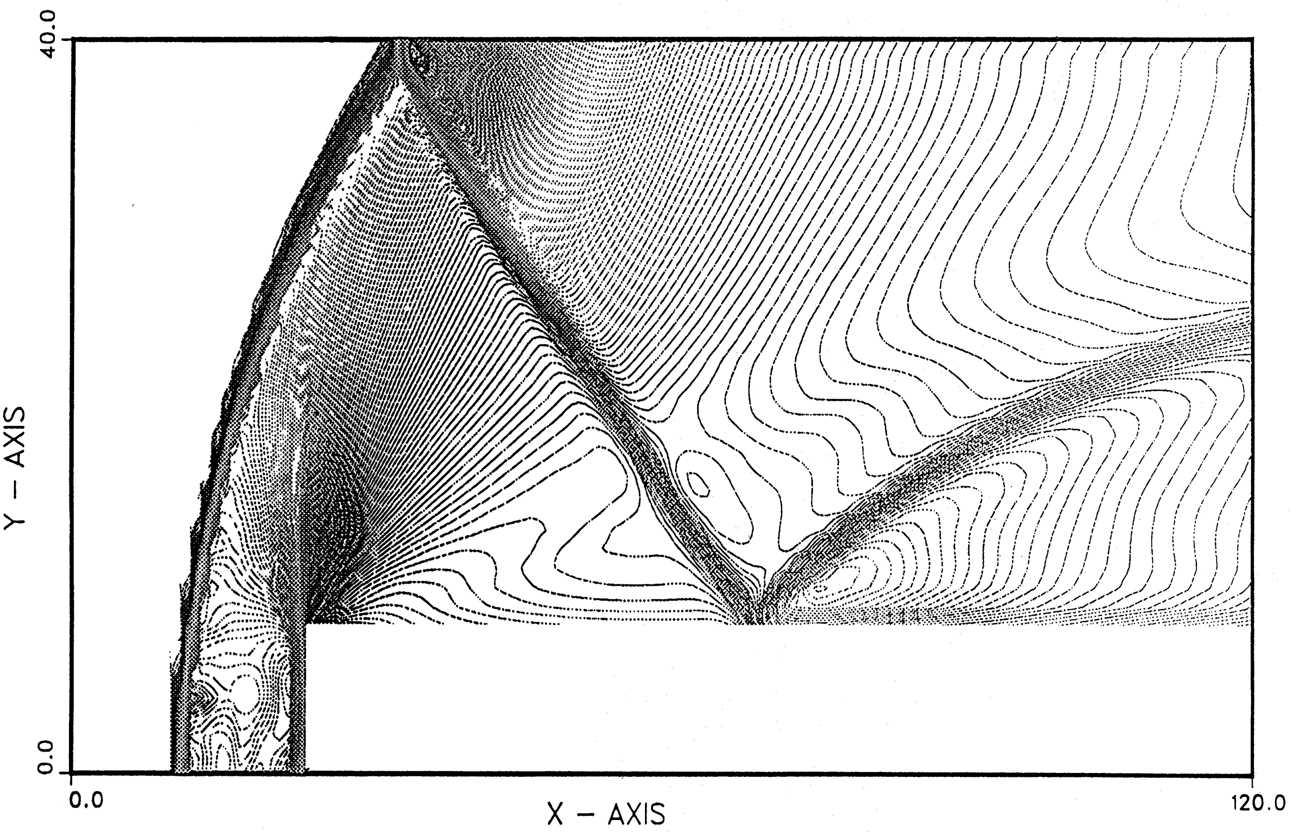

Fig. 5. Relativistic Emery's step. Isodensity curves at $t = 6$, in units of the Courant time

Table 2. Jacobian matrices. a, b, c stand for the components of the three-velocity v^x, v^y, v^z, respectively.

$$\mathcal{A}^0 = \begin{bmatrix} W & \rho aW^3 & \rho bW^3 & \rho cW^3 & 0 \\ (1+\epsilon+\chi)aW^2 & \rho hW^2(1+2a^2W^2) & 2\rho habW^4 & 2\rho hacW^4 & (\rho+\kappa)aW^2 \\ (1+\epsilon+\chi)bW^2 & 2\rho habW^4 & \rho hW^2(1+2b^2W^2) & 2\rho hbcW^4 & (\rho+\kappa)bW^2 \\ (1+\epsilon+\chi)cW^2 & 2\rho hacW^4 & 2\rho hbcW^4 & \rho hW^2(1+2c^2W^2) & (\rho+\kappa)cW^2 \\ (1+\epsilon+\chi)W^2-\chi-W & 2\rho haW^4-\rho aW^3 & 2\rho hbW^4-\rho bW^3 & 2\rho hcW^4-\rho cW^3 & (\rho+\kappa)W^2-\kappa \end{bmatrix}$$

$$\mathcal{A}^1 = \begin{bmatrix} aW & \rho W(1+a^2W^2) & \rho abW^3 & \rho acW^3 & 0 \\ (1+\epsilon+\chi)a^2W^2+\chi & 2\rho haW^2(1+a^2W^2) & 2\rho ha^2bW^4 & 2\rho ha^2cW^4 & (\rho+\kappa)a^2W^2+\kappa \\ (1+\epsilon+\chi)abW^2 & \rho hbW^2(1+2a^2W^2) & \rho haW^2(1+2b2W^2) & 2\rho habcW^4 & (\rho+\kappa)abW^2 \\ (1+\epsilon+\chi)acW^2 & \rho hcW^2(1+2a^2W^2) & 2\rho habcW^4 & \rho haW^2(1+2c^2W^2) & (\rho+\kappa)acW^2 \\ (1+\epsilon+\chi)aW^2-aW & \rho hW^2(1+2a^2W^2)-\rho W(1+a^2W^2) & 2\rho habW^4-\rho abW^3 & 2\rho hacW^4-\rho acW^3 & (\rho+\kappa)aW^2 \end{bmatrix}$$

$$\mathcal{A}2 = \begin{bmatrix} bW & \rho abW^3 & \rho W(1+b^2W^2) & \rho bcW^3 & 0 \\ (1+\epsilon+\chi)abW^2 & \rho hbW^2(1+2a^2W^2) & \rho haW^2(1+2b^2W^2) & 2\rho habcW^4 & (\rho+\kappa)abW^2 \\ (1+\epsilon+\chi)b^2W^2+\chi & 2\rho hab^2W^4 & 2\rho hbW^2(1+b^2W^2) & 2\rho hb^2cW^4 & (\rho+\kappa)b^2W^2+\kappa \\ (1+\epsilon+\chi)bcW^2 & 2\rho habcW^4 & \rho hcW^2(1+2b^2W^2) & \rho hbW^2(1+2c^2W^2) & (\rho+\kappa)bcW^2 \\ (1+\epsilon+\chi)bW^2-bW & 2\rho habW^4-\rho abW^3 & \rho hW^2(1+2b^2W^2)-\rho W(1+b2W^2) & 2\rho hbcW^4-\rho bcW^3 & (\rho+\kappa)bW^2 \end{bmatrix}$$

$$\mathcal{A}^3 = \begin{bmatrix} cW & \rho acW^3 & \rho bcW^3 & \rho W(1+c^2W^2) & 0 \\ (1+\epsilon+\chi)acW^2 & \rho hcW^2(1+2a^2W^2) & 2\rho habcW^4 & \rho haW^2(1+2c^2W^2) & (\rho+\kappa)acW^2 \\ (1+\epsilon+\chi)bcW^2 & 2\rho habcW^4 & \rho hcW^2(1+2b^2W^2) & \rho hbW^2(1+2c^2W^2) & (\rho+\kappa)bcW^2 \\ (1+\epsilon+\chi)c^2W^2+\chi & 2\rho hac^2W^4 & 2\rho hbc^2W^4 & 2\rho hcW^2(1+c^2W^2) & (\rho+\kappa)c^2W^2+\kappa \\ (1+\epsilon+\chi)cW^2-cW & 2\rho hacW^4-\rho acW^3 & 2\rho hbcW^4-\rho bcW^3 & \rho hW^2(1+2c^2W^2)-\rho W(1+c^2W^2) & (\rho+\kappa)cW^2 \end{bmatrix}$$

hibits the most complex structure. The main features of the solution are the Mach reflection of a *bow shock* at the upper wall, making the density distribution the most difficult to compute, and a *rarefaction fan* centered at the corner of the step. These general characteristics of the solution are similar to those found in the Newtonian case. Currently, we are experimenting with higher inflow velocities.

5. Concluding remarks

In this paper, we have derived the spectral decomposition of the Jacobian matrices associated to the fluxes of the three-dimensional special relativistic hydrodynamics system of equations and discussed the interest of this analysis, both from the theoretical and from the numerical point of view.

In this way, we have set out the theoretical ingredients which are necessary in order to use modern high-resolution shock-capturing methods in multidimensional relativistic hydrodynamics.

Our relativistic multidimensional hydro-code, which is the natural extension of previous work in the one-dimensional case, has overcome two severe tests: a steady relativistic oblique shock and Emery's problem. For the first test there are analytical relations which allow us to compare the numerical results with the theoretical ones. The severe test of Emery's step is a standard one (in its Newtonian version) due to their richness in structures – shocks, rarefactions,... – which are challenging for a multidimensional relativistic hydro-code.

The results obtained in the above mentioned tests, give us confidence in the feasibility of our procedure for extending modern high-resolution shock-capturing methods to the multidimensional relativistic hydrodynamics.

Acknowledgements. This work has been supported by the Spanish DGICYT (grants PB91-0648 and PS90-0265). José Mª. Martí has benefited from a postdoctoral fellowship of the Ministerio de Educación y Ciencia (MEC). Calculations were carried out in a VAX 6000/410 at the Instituto de Física Corpuscular and in a IBM 30-9021 VF at the Centre de Informàtica de la Universitat de València. One of us (J.M.M.) is thankful to G. Mellema for providing a very recent preprint.

Appendix A: Jacobian matrices

The Jacobian matrices $\mathcal{A}^\alpha$ introduced in (13) are displayed in Table 2. Note that the above matrices verify:

(1) $\mathcal{A}^2 = \mathcal{P}_{21}[\mathcal{A}^1]$,
(2) $\mathcal{A}^3 = \mathcal{P}_{31}[\mathcal{A}^1]$,
(3) $\mathcal{A}^0 = \mathcal{P}_{21}[\mathcal{A}^0] = \mathcal{P}_{31}[\mathcal{A}^0]$,

where operators $\mathcal{P}_{q1}$ $(q = 2, 3)$ act on their arguments as defined by the following sequential operations:

(1) To permute the second and $(q+1)$th arrows.
(2) To permute the second and $(q+1)$th columns.
(3) To interchange the velocity components v^x and v^q.

Appendix B: mathematical details

Let us point out the connection between the spectral decomposition of the eigenvalue problem (23) and the Jacobian matrices $\mathcal{B}^i$ associated to system (17).

Let $\mathcal{D}(\lambda)$ and $\mathcal{D}^*(\lambda)$ be 5×5-matrices defined by

$$\mathcal{D}(\lambda) = \mathcal{A} - \lambda\mathcal{A}^0 , \tag{37}$$

$$\mathcal{D}^*(\lambda) = \mathcal{A}(\mathcal{A}^0)^{-1} - \lambda\mathcal{I} , \tag{38}$$

where $\mathcal{A}$ is one of the matrices $\mathcal{A}^i$ introduced in (13).

Having in mind that $\mathcal{A}^0$ is nonsingular, it is easy to check that

$$\det[\mathcal{D}(\lambda)] = det[\mathcal{D}^*(\lambda)]\det(\mathcal{A}^0) . \tag{39}$$

This relation establishes that the equations,

$$\det\mathcal{D}(\lambda) = 0 , \tag{40}$$

$$\det\mathcal{D}^*(\lambda) = 0 , \tag{41}$$

have the same solution for the eigenvalue λ. Then, if $\{\lambda_n\}_{n=1,...5}$ and $\{\lambda^*_n\}_{n=1,...5}$ are the sets of eigenvalues corresponding to the characteristic Eqs. (40) and (41) we have proved that

$$\{\lambda_n\}_{n=1,...5} = \{\lambda^*_n\}_{n=1,...5} . \tag{42}$$

Now, let λ_n be one of this eigenvalues and let $\boldsymbol{r}_n$ be one vector satisfying $\mathcal{D}(\lambda_n)\boldsymbol{r}_n = 0$. Writing this expression explicitly and taking $\mathcal{A}^0$ as common factor, we have

$$[\mathcal{A}(\mathcal{A}^0)^{-1} - \lambda_n\mathcal{I}]\mathcal{A}^0\boldsymbol{r}_n = 0 . \tag{43}$$

On the other hand, the set of eigenvectors of $\mathcal{A}(\mathcal{A}^0)^{-1}$, $\{\boldsymbol{r}^*_n\}_{n=1,...5}$, are, by definition, those verifying

$$[\mathcal{A}(\mathcal{A}^0)^{-1} - \lambda^*_n\mathcal{I})\boldsymbol{r}^*_n = 0 . \tag{44}$$

Comparison of expressions (43) and (44), considering that (42) holds, shows that

$$\{\boldsymbol{r}^*_n\}_{n=1,...5} = \{\mathcal{A}^0\boldsymbol{r}r_n\}_{n=1,...5} \tag{45}$$

exception made of a normalization factor.

Let us note that this result guarantees that a state $\boldsymbol{w}$ is a weak solution to (8) if and only if the corresponding vector $\boldsymbol{u}$, given by (15), is a weak solution of (17).

References

Anile A.M., 1989, Relativistic Fluids and Magneto-Fluids. Cambridge University Press, Cambridge
Begelman M.C., Blandford R.D., Rees M.J., 1984, Rev. Mod. Phys. 56, 255
Brown G.E., Bethe H.A., Baym G., 1982, Nucl. Phys. A375, 481
Centrella J., Wilson J.R., 1984, ApJS 54, 229
Dubal M.R., 1991, Comput. Phys. Commun. 64, 221
Emery A.F., 1968, J. Comput. Phys. 2, 306

Eulderink F., Mellema G., 1993, STW 211-92, A&A (preprint)
Evans C. R., 1986, in: Cantrella J. (ed.) Dynamical Space-Times and Numerical Relativity. Cambridge University Press, Cambridge
Friedrichs K.O., 1974, Commun. Pure Appl. Math. 27, 749
Godunov S.K., 1959, Matematicheskii Sbornik 47, 271
Harten A., 1983, J. Comput. Phys. 49, 357
Harten A., Hyman J.M., 1983, J. Comput. Phys. 50, 235
Hawley J.F., Smarr L. L., Wilson J. R., 1984, ApJ 277, 296
Königl A., 1980, Phys. Fluids 23, 1083
Ibáñez J.Mª., 1993, Invited talk given at the Summer Course on Gravitation and General Relativity, held at El Escorial, Spain, August 1992. To appear in Lecture Notes in Physics, Springer, Berlin
Lax P., 1973, Regional Conference Series Lectures in Applied Math., Vol. 11, SIAM, Philadelphia, PA
LeVeque R.J., 1991, Numerical Methods for Conservation Laws, Birkhäuser, Basel
Mann P.J., 1991, Comput. Phys. Commun. 67, 245
Marquina A., Martí J.Mª., Ibáñez J.Mª., Miralles J.A., Donat R., 1992, A&A 258, 566
Martí J.Mª., Ibáñez J.Mª., Miralles J.A., 1991, Phys. Rev. D43, 3794 (MIM)
Miller J.C., Pantano O., 1989, Phys. Rev. D40, 1789
Nakamura T., 1981, Prog. Theor. Phys. 65, 1876
Nakamura T., Maeda K., Miyama S., Sasaki M., 1980, Prog. Theor. Phys. 63, 1229
Nakamura T., Sato H., 1982, Prog. Theor. Phys. 67, 1396
Osher S., 1985, SIAM J. Num. Anal. 22, 947
Piran T., 1980, J. Comput. Phys. 35, 254
Shapiro S.L., Teukolsky S.A., 1983, Black Holes, White Dwarfs and Neutron Stars. Wiley, New York
Shu C.W., Osher S., 1989, J. Comput. Phys. 83, 32
Sod G.A., 1987, Numerical Methods in Fluid Dynamics. Cambridge University Press, Cambridge
Stark R.F., Piran T., 1987, Comput. Phys. Rept. 5, 221
Strottman D., 1989, in: Greiner W., Stöcker H. (eds.) The Nuclear Equation of State, Part B. Plenum Press, New York
Taussig R., 1973, in: Lighthill M.J., Imai I., Sato H. (eds.) Dynamics of Ionized Gases. Tokyo University Press, Tokyo
Van Leer B., 1979, J. Comput. Phys. 32, 101
Wilson J.R., 1972, ApJ 173, 431
Wilson J.R., 1979, in: L.L. Smarr (ed.) Sources of Gravitational Radiation. Cambridge University Press, Cambridge
Wilson M.J., 1987, MNRAS 226, 447
Yee H.C., 1989, VKI Lecture Notes in Computational Fluid Dynamics, von Karman Institute for Fluid Dynamics